

Luke BERGLIND^{1*}
John ZIEGERT¹

ANALYTICAL TIME-DOMAIN MODEL FOR TOOL POINT DYNAMICS IN TURNING

An analytical time domain solution is developed to model the dynamic response of a tool during a simple turning operation. The time domain solution developed in this paper relies on the superposition principle under the linear assumption to construct the time response of single mode, single degree of freedom cutting tool. The results from the analytical solution are compared with those generated using numerical time domain simulations and it is found that the two solutions converge as the time step used in the numerical simulation decreases.

1. INTRODUCTION

Dynamic instability, or chatter, is a common occurrence in machining environments which can lead to undesirable part outcomes in terms of part surface and dimensional quality. Chatter is a result of regenerative dynamic forces inherent in the machining process which can cause the system to be either stable or unstable depending on the parameters of the cutting operation and the dynamic characteristics of the machine tool [9],[12]. One of the primary objectives of research in machine dynamics is to better understand and characterize the dynamic behavior of machining operations so that chatter can be avoided.

The first successful model for machine tool chatter for turning is based on the concept of regenerative vibrations developed by Tlusty in [9]. In this model, force interactions between the vibrations of the tool during one pass and the imprinted surface left behind in the previous pass cause the tool to be either stable or unstable depending on the dynamic properties of the tool and the cutting parameters. Due to the influence of the tool motion during the previous pass, a delay differential equation (DDE) is required to describe the system dynamics. Due to the difficulty in solving the DDE analytically, the limiting stable depth of cut over a range of spindle speeds is determined by examining the vibration magnitudes of subsequent passes in the frequency domain.

The methods developed by Tlusty continue to be effective for continuous cutting

¹ UNCC, Faculty of Mechanical Engineering, Charlotte, NC, USA

* E-mail: lberglin@uncc.edu

applications (like turning) even when compared with more recently developed stability analyses methods [2]. However, increased complexity of the cutting processes in milling have motivated further research in stability analysis methods for milling applications. Using a similar approach developed by Tlustý for turning, others have expanded the technique by incorporating various levels of detail on the varying directional force coefficients present in milling to increase the accuracy of the stability lobes [1],[6]. Insperger and Stepan developed an alternative stability analysis technique in which the DDE describing the system is converted to a periodic DDE, and the Floquet Theorem is applicable to determine stability[4],[5].

Time domain simulations are also effective in analyzing the stability of machine tool stability. Numerical simulations are advantageous because they easily account for nonlinearities in the system, such as varying force directions and loss of contact between the tool and the work-piece [11]. However, the high fidelity of the time marching numerical simulations comes at high computational expense. Furthermore, the results of numerical simulations only indicate whether the system is stable or unstable, and there is no indication as to the underlying cause of the behavior.

To improve the efficiency of stability analysis in the time domain, Davies et al. developed an analytical approach where the tool point dynamics are derived using two separate models depending on whether the tool is in or out of the cut during low radial immersion milling [2],[3]. While the analytical solution for the free, non-cutting tool is trivial, the analytical solution for the tool in the cut is approximated as an impulse [3] or using temporal finite element analysis [2] because there is no exact solution during cutting.

In this paper an analytical solution is developed to solve for the time response of the DDE in the regenerative chatter model. In this solution, the propagating effects of some perturbation event are determined analytically, independent of the time delay. Through superposition, these propagating effects are combined to form the total time response of the tool for a single degree of freedom system. The effectiveness of the analytical solution is determined by comparing the time responses to those obtained using numerical simulations of a turning operation.

2. DYNAMIC MODEL

The model used to develop the time domain solution is shown in Fig. 1. The tool is modeled as a single mode, single degree of freedom spring mass damper system which is flexible in the feed direction of the tool. The forcing function which acts on the tool during the cutting operation is derived by assuming orthogonal cutting conditions. Under the orthogonal cutting assumption, the tool face is oriented normal to the feed direction, and the magnitude of the cutting force, F , is found as the product of the chip area (area of contact between the tool and the material), and the material cutting force constant, K_s . The dominant cutting forces are in the direction of the material flow (F_t), and the feed direction (F_n), which are related to the force magnitude, F , through a cutting force angle, β . As the tool is assumed to be flexible only in the feed direction, only the normal component of the force, F_n , affects tool motions. The cutting force constant, K_s , and the cutting force angle,

β , are determined experimentally, and the chip area is calculated as the product of the instantaneous chip thickness, $h(t)$, and the depth of cut, b (the depth of cut, b , is in the out of plane direction in Fig. 1).

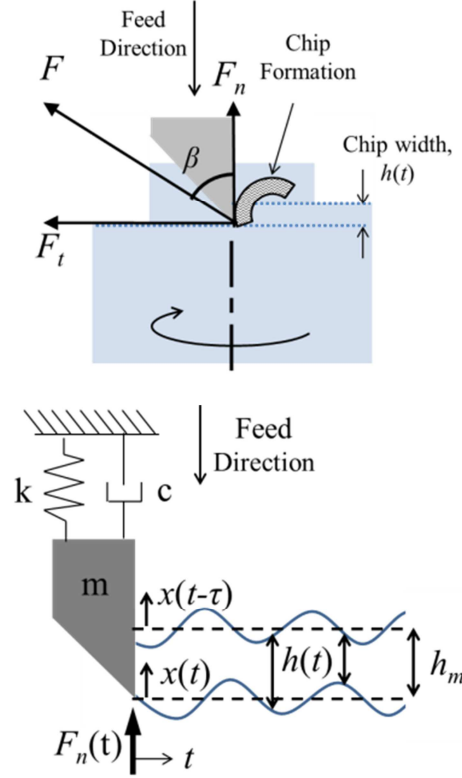


Fig. 1. Illustration of cutting forces acting on the tool during orthogonal cutting, and the variation in the chip thickness, $h(t)$

The resulting force acting on the tool varies over time due to variability in the chip area caused by changes in the chip thickness, $h(t)$. The chip thickness describes the dimension of the chip area in the direction in which the tool is flexible, as such, tool point vibrations change the effective area of the chip, and leave a wavy surface on the part. The resulting value of the chip thickness, $h(t)$, is then a function of the tool position in the current pass, $x(t)$, the tool position in the previous pass, $x(t-\tau)$, and the global feed per revolution, h_m . The resulting expressions describing the force which acts on the tool, F_n , and the instantaneous chip thickness, h , are shown in equations (1) and (2). The resulting differential equation describing the tool point dynamics in turning process is shown in equation (3).

$$F_n(t) = K_s \cos(\beta) b h(t) \quad (1)$$

$$h(t) = h_m + x(t-\tau) - x(t) \quad (2)$$

$$m\ddot{x} + c\dot{x} + kx = K_s \cos(\beta) b (h_m + x(t-\tau) - x(t)) \quad (3)$$

3. GENERAL ANALYTICAL APPROACH

The time delay term, τ , in equation (3) is required to describe the system dynamics because the instantaneous cutting force is dependent on the tool position during the previous revolution. The resulting time delay differential equation (DDE) significantly increases the complexity for an analytical time domain solution. Before delving into the processes used to solve equation (3) in particular, we will first discuss the general solution strategies for problems of this type.

The method of steps [7] is the most common approach to solve DDEs of this form (linear with a single, discrete time delay). This method has been used to develop a time domain solution for turning in [8], however, the solution process proved to be extremely cumbersome after only a few part revolutions, and a Matlab solver, dde23 [10], was employed to simulate the tool behavior over longer periods of time. In this paper an alternative approach used to solve equation (3) which uses superposition to simplify the solution process. The two solution approaches are compared by examining a simple DDE example shown in equation (4).

$$y' + y(t - \tau) = 0, \quad y(0) = 1, \quad y_0 = 1 \quad (4)$$

The method of steps solves DDEs by replacing the delay term, $y(t - \tau)$, with a known function which defines y over the previous time interval, $(n-1)\tau \leq t < n\tau$, starting with an initial function, y_0 , defining the position on $-\tau \leq t < 0$ to start the solution process. By replacing the delay term with a known function, the DDE is converted into an ordinary differential equation (ODE) that can be solved over discrete time periods. The general solution procedure is shown in equation (5), where the solution over the interval, $n\tau \leq t < (n+1)\tau$, is the solution to equation (5) when the position from the previous interval, y_n , is the input. The initial condition at the start of each new interval is equal to the condition of the system at the end of the previous range. In this way, the total solution is found as a set of individual solutions, each defined over a discrete time interval. The solution to equation (4) using the method of steps with a time delay of $\tau = 0.5$ s is shown in Fig. 2. Each interval in Fig. 2 is defined by a single function, $y_n(t)$, and the function for each interval defines the negative slope of the following interval.

$$\begin{aligned} y'_{n+1}(t) &= -y_n(t), \quad n\tau \leq t < (n+1)\tau, \\ y_{n+1}(n\tau) &= y_n(n\tau) \end{aligned} \quad (5)$$

The approach developed in this paper to solve equation (3) is similar to the method of steps in that it converts the single DDE into multiple ODEs. However, rather than having a separate function describing the response over each individual time interval, superposition is used to construct the total response using a set of individual solution curves, called sequential responses. The sequential responses, $y_j(t)$, used to form the solution to equation (4) are found by solving the recursive differential equation shown in equation (6). Note that the sequential responses are defined on a range of zero to infinity, and the initial condition is always zero. In equation (7) the first four sequential responses are calculated according to

equation (6), starting with the initial function, $y_0 = 1$ starting at $t = -\tau$. Based on the patterns that emerge from the recursive solutions, the expression for any sequential response for this problem can be calculated directly using equation (8).

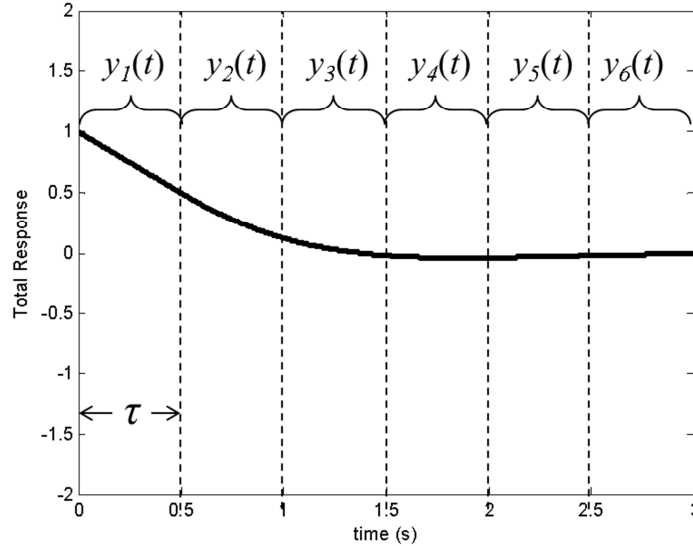


Fig. 2. Solution to equation (4) using the method of steps with a time delay of $\tau = 0.5$ s

$$y'_j(t) = -y_{j-1}(t), \quad 0 \leq t < \infty, \quad y_j(0) = 0 \quad (6)$$

$$\begin{aligned} y_0 &= 1 \\ y'_1 &= -y_0 = -1 \quad \rightarrow \quad y_1 = -t \\ y'_2 &= -y_1 = t \quad \rightarrow \quad y_2 = \frac{t^2}{2} \end{aligned} \quad (7)$$

$$y'_3 = -y_2 = -\frac{t^2}{2} \quad \rightarrow \quad y_3 = -\frac{t^3}{6}$$

$$y'_4 = -y_3 = \frac{t^3}{6} \quad \rightarrow \quad y_4 = \frac{t^4}{24}$$

$$y_j = \frac{(-1)^j t^j}{j!} \quad (8)$$

The sequential responses described by equation (8) form a basic set of curves which combine through superposition to form the total solution to equation (4). To form the solution to the DDE, each sequential response is added to the total solution at a delayed time, such that the sequential response, y_j , starts at time $t=(j-1)\tau$. The structure of the total solution is defined in equation (9) and a depiction of the process is shown in Fig. 3. Note that the value of each sequential response is zero at the time which it is added to the total solution. This is due to the zero initial condition established in equation (6) which prevents discontinuities in the total response (i.e. the conditions at the start of each time interval in the method of steps is already accounted for by the previous sequential responses in the superposition approach).

$$y(t) = \sum_{j=0}^{\infty} \begin{cases} 0 & , t < \tau(j-1) \\ y_j(t - \tau(j-1)) & , t \geq \tau(j-1) \end{cases} \quad (9)$$

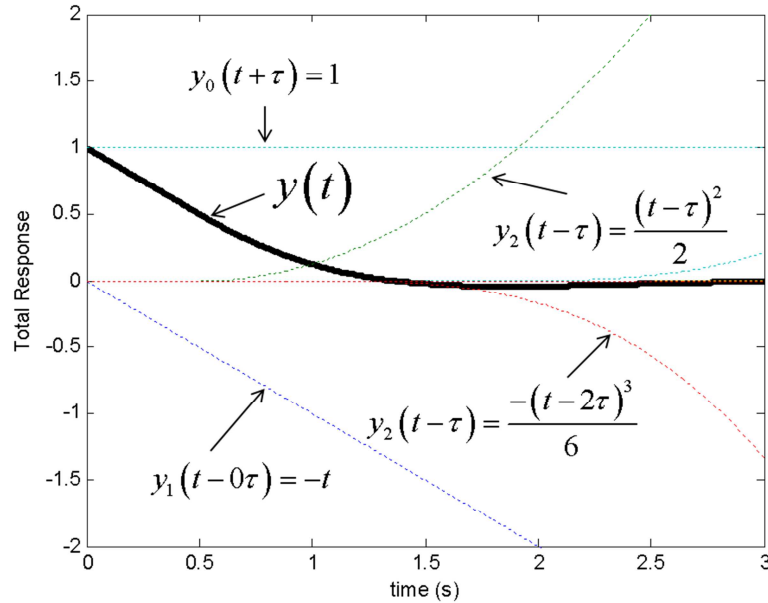


Fig. 3. Illustration of how the total solution is constructed using the sequential responses

It is also interesting to note that as the delay approaches zero, the total response described by equation (8) and (9) reduces to equation (10). The resulting summation is the series definition of e^{-t} , which is known to be the solution to $y' + y(t-0) = 0$.

$$y(t) = \sum_{j=0}^{\infty} y_j = \sum_{j=0}^{\infty} \frac{(-1)^j t^j}{j!} = e^{-t} \quad (10)$$

What is most significant about the superposition approach is that the sequential responses which constitute the total response of the system are independent of the time delay term. As such, for a given system the sequential responses need only be derived once, and the total response can be determined for different values of τ by changing where in time the individual sequential responses are applied. For example, in Fig. 4 the solution to equation (4) using the superposition approach is shown for four different time delays. Each solution shows significantly different behavior, however, the sequential responses which constitute the total solutions are the same in each. This is in contrast with the method of steps, where the individual functions for each time interval, y_n , must be re-calculated if τ is changed. The general process discussed here to solve linear DDEs with a single discrete time delay is now applied to the more complicated turning process. In the following sections, equation (3) is modified to a form in which the superposition approach can be applied, and the resulting sequential responses for turning are derived. These sequential responses are then combined with different time delays to produce the total time response of the tool during the turning process.

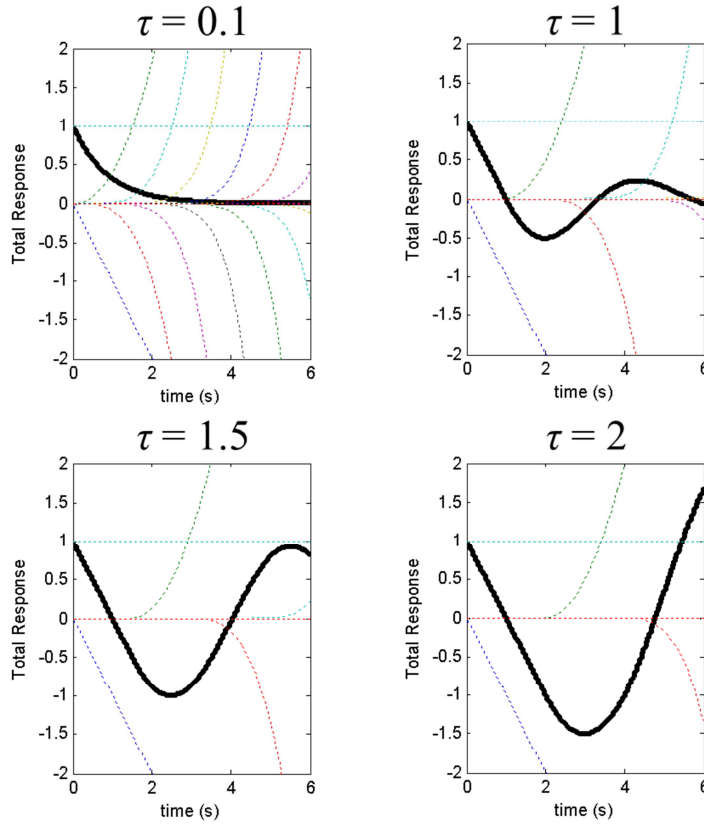


Fig. 4. Sequential responses used to solve equation (4) for multiple delays, where the sequential responses are the same for each solution

4. ANALYTICAL TURNING MODEL

The solution process for equation (3) begins by assuming that the chip profile that the tool encounters at any point in time, $h_{nom}(t)$, is known. The nominal chip profile, shown in Fig. 5, includes information about the tool motions in the previous pass relative to the neutral position of the tool, $x(t) = 0$. If the chip profile, $h_{nom}(t)$, is known, then the resulting force on the tool at any point in time can be calculated as $F_n = bR(h_{nom}(t) - x(t))$, where $R = K_s \cos(\beta)$. Substituting the modified force expression into equation (3), and moving the remaining x term in the forcing function to the left side of the equation, the resulting ODE describing the tool point response is given in equation (11), where $k_p = k + bR$.

$$m\ddot{x} + c\dot{x} + k_p x = bR h_{nom}(t) \quad (11)$$

The resulting ODE successfully eliminates the time delay term in equation (3) because it is assumed that the chip profile, including information about the tool position in the previous pass, is known. The objective of the superposition approach is to predict the chip profile, $h_{nom}(t)$, that the tool will encounter based on the action of the tool during all prior passes.

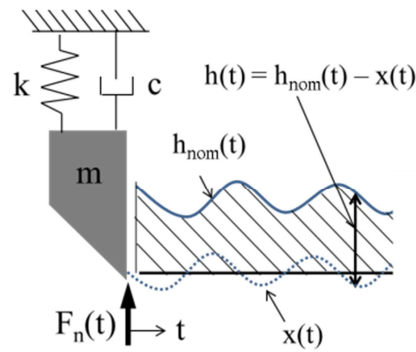


Fig. 5. Modified view of the chip profile, where the nominal chip profile, $h_{nom}(t)$ is known

In order to predict the nominal chip profile, the initial stages of the turning process are examined. In Fig. 6 the initial stages of a turning operation are shown, where the tool feeds into a part which initially has a flat face. During the first rotation the nominal chip profile increases linearly, and then flattens out at the end of the first rotation when the tool encounters material removed during the first revolution.

The initial nominal chip profile in Fig. 6 can be modelled as a combination of two ramp functions, shown as $h_{nom,1}(t)$ and $-h_{nom,1}(t)$ in Fig. 7. The first ramp function begins at $t=0$ and represents the tool feeding into the part during the first rotation. The second is a negative ramp function beginning at $t=\tau$ with the same slope as the first which causes the total input to flatten out at $t=\tau$. Under the linear assumption, the total response of the tool can be found as the summation of the responses to the two individual ramp input functions. The individual responses, $x_1(t)$ and $-x_1(t)$, are the solutions to equation (11) when $h_{nom,1}(t)$ and $-h_{nom,1}(t)$ are input. The total response, $x(t)$ in Fig. 7, is then the summation of $x_1(t)$ and $-x_1(t)$, where $x_1(t)$ starts at $t=0$, and $-x_1(t)$ starts at $t=\tau$.

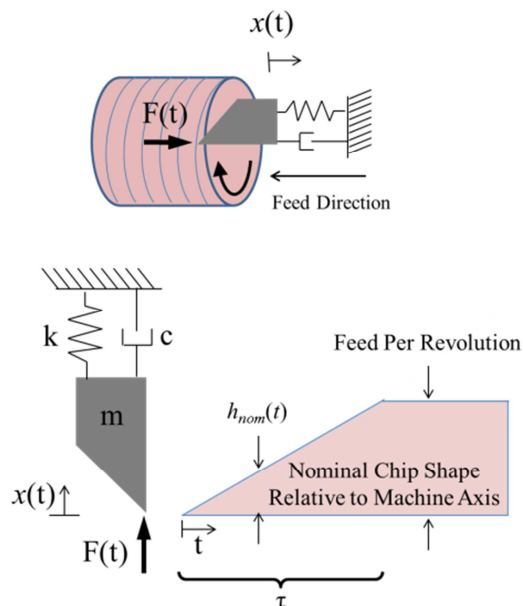


Fig. 6. Illustration of the beginning of the turning operation, and the nominal chip profile shape that the tool will encounter

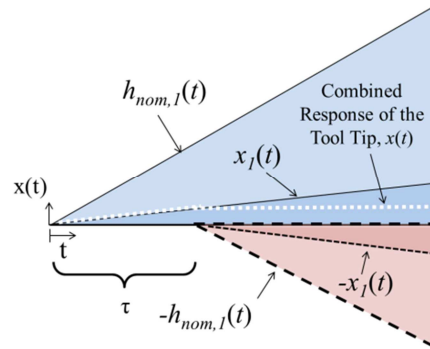


Fig. 7. Superposition used to model the initial nominal chip profile as a combination of two ramp functions, separated by time, τ

The next step is to consider the material that was left behind during the first rotation that the tool will again encounter during the second rotation, as shown in Fig. 8. Fortunately, this additional material profile is known exactly as $x_1(t)$. Superposition is again applied to append the effects of the material left behind in the first rotation starting at the beginning of the second rotation. This additional response, $x_2(t)$ starting at $t=\tau$, is found by solving equation (11) using $h_{nom,2}(t)=x_1(t)$ as the input function. Finally, the total response for the second part rotation is calculated as the summation of $x_1(t)$ starting at $t=0$, and $x_2(t)-x_1(t)$ starting at $t=\tau$, as shown in Fig. 8.

$$x(t) = x_1(t) + \sum_{j=2}^N \begin{cases} 0 & , t < (j-1)\tau \\ x_j(t - (j-1)\tau) - x_{j-1}(t - (j-1)\tau) & , t \geq (j-1)\tau \end{cases} \quad (12)$$

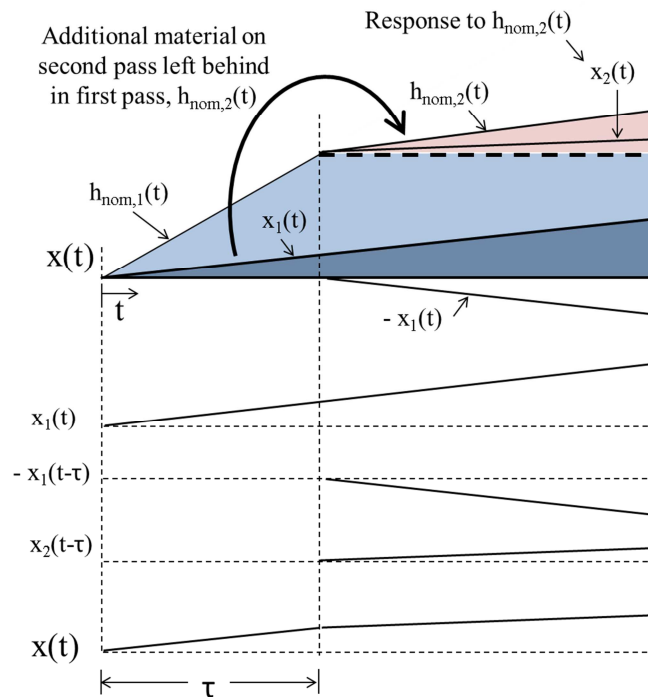


Fig. 8. Superposition used to model the influence of the material left behind in the first part rotation

As the number of rotations increases, the same process is repeated, where the subsequent responses, $x_j(t)$ and $-x_{j-1}(t)$, are applied to the total response of the system starting at $t = (j-1)\tau$. The resulting time domain response for the turning operation shown in Fig. 6 is given in equation (12), where N is the total number of part rotations, and $x_j(t)$ is the j th sequential response to the initial ramp input.

5. SEQUENTIAL RESPONSES

The sequential responses, $x_j(t)$ in equation (12), which combine to form the total tool response for the turning process are derived by modelling repeated tool passes over the same section of material starting with an initial ramp profile. Looking at Fig. 8, the response to the material left in the first revolution is calculated by solving equation (11) with the input function, $h_{nom,2}(t)=x_1(t)$, to obtain $x_2(t)$. For the third revolution, the additional material left behind during the second revolution must then be accounted for by solving equation (11) with the input function, $h_{nom,3}(t)=x_2(t)$, to obtain $x_3(t)$, and so on. This process is illustrated in Fig. 9, where the sequential responses are found as the response of the tool as it passes over the material left behind in the previous pass.

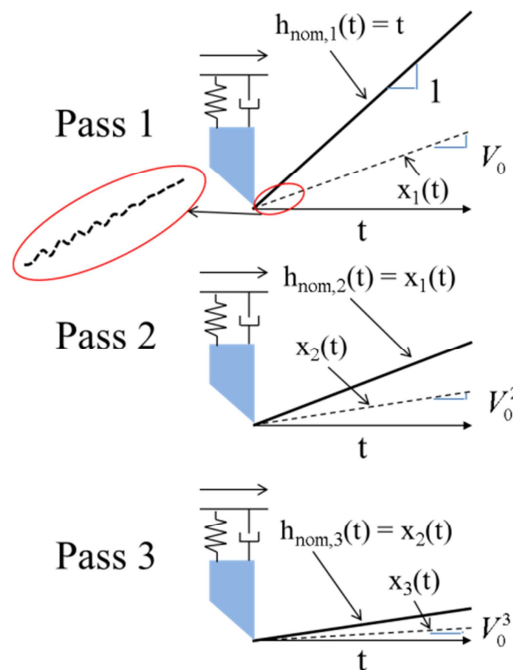


Fig. 9. illustration of how the sequential responses are calculated, starting with an initial ramp function

The analytical representation of the sequential responses is expressed in equation (13) as a recursive differential equation. The base function which begins the sequential responses is a linear function of slope one, $x_0(t)=t$. Note that the actual slope of the initial function is equal to $(\text{RPM}) \cdot (\text{Feed per rev}) / 60$, which reflects the rate which the tool feeds into the part.

The initial slope of one is used here to simplify calculations of the sequential responses. After calculation, the responses are scaled to reflect the actual slope. Additionally, the initial conditions for the tool at the beginning of each sequential response are zero velocity and zero displacement. When the sequential responses are added to the total solution, at time $t=(j-\tau)$ according to equation (12), the tool is already following a motion path that is defined in the previous revolutions. As such, the conditions of the tool at the start of a new revolution are already accounted for, and zero initial conditions can be applied to find the influence of the material left in the previous pass.

$$\begin{aligned} m\ddot{x}_j + c\dot{x}_j + k_p x_j &= bR x_{j-1} \\ x_0(t) = t, \quad x_j(0) &= 0, \quad \dot{x}_j(0) = 0 \end{aligned} \quad (13)$$

5.1. CALCULATION OF SEQUENTIAL RESPONSES

The first sequential response is calculated by applying the input, $x_0(t)=t$, into equation (13) and solving for the response, $x_1(t)$. The resulting expression for the first sequential response is shown in equation (14).

$$\begin{aligned} x_1(t) &= V_0 \left(\overbrace{e^{-At} \left(\frac{1}{\omega_p} \left(\frac{cA}{k_p} - 1 \right) \sin(\omega_p t) + \frac{c}{k_p} \cos(\omega_p t) \right)}^{AC} + \overbrace{t - \frac{c}{k_p}}^{\text{Linear, DC}} \right) \\ A &= \frac{c}{2m}, \quad \omega_p = \sqrt{\frac{k_p}{m} - A^2}, \quad V_0 = \frac{bR}{k_p} \end{aligned} \quad (14)$$

where ω_p is the damped natural frequency of the system, A is the exponential decay term for the tool vibrations and V_0 is the slope of the response relative to the slope of the initial input function. The second sequential response is then found by inputting $x_1(t)$ from equation (14) into equation (13), and solving for $x_2(t)$. Expressions for the first three sequential responses are shown in equation (15) after substituting $H = \frac{c}{k_p}$, $G = \frac{1}{\omega_p}(HA-1)$.

The resulting plots for the first three sequential responses in equation (15) are shown in Fig. 10 for the system parameters defined in Table 1. It can be seen that each response is composed primarily of vibrational and linear components, and that the slopes of the linear components, which dominate the early responses, decrease significantly as the number of responses increases. Eventually, the linear component effectively diminishes and the vibration component dominates. In Fig. 11 the vibration components of the first three sequential responses are plotted. The vibrations of each response are a result of excitation from the vibrations of the previous response, and it is the behavior of these subsequent vibrations and their interactions through equation (12) which determines the behavior of the total response.

$$\begin{aligned}
x_1(t) &= V_0 e^{-At} (G \sin(\omega_p t) + H \cos(\omega_p t)) + V_0 (t - H), \\
x_2(t) &= V_0 \left(\frac{bR}{m} \right) e^{-At} \left[\begin{aligned} &\frac{G}{2\omega_p} t \sin\left(\omega_p t - \frac{\pi}{2}\right) + \frac{H}{2\omega_p} t \cos\left(\omega_p t - \frac{\pi}{2}\right) \\ &+ \left(\frac{G}{2\omega_p^2} + \frac{m}{\omega_p k_p} \right) \sin(\omega_p t) + 2H \frac{m}{k_p} \cos(\omega_p t) \end{aligned} \right] + V_0^2 (t - 2H), \\
x_3(t) &= V_0 \left(\frac{bR}{m} \right)^2 e^{-At} \left[\begin{aligned} &\frac{G}{8\omega_p^2} t^2 \sin\left(\omega_p t - 2\frac{\pi}{2}\right) \\ &+ \frac{H}{8\omega_p^2} t^2 \cos\left(\omega_p t - 2\frac{\pi}{2}\right) \\ &+ \frac{1}{2\omega_p} \left(\frac{3G}{4\omega_p^2} + \frac{m}{\omega_p k_p} \right) t \sin\left(\omega_p t - \frac{\pi}{2}\right) \\ &+ \frac{1}{2\omega_p} \left(\frac{H}{4\omega_p^2} + 2H \frac{m}{k_p} \right) t \cos\left(\omega_p t - \frac{\pi}{2}\right) \\ &+ \left(\frac{1}{2\omega_p} \left(\frac{3G}{4\omega_p^2} + \frac{m}{\omega_p k_p} \right) - \frac{1}{\omega_p} \left(\frac{m}{k_p} \right)^2 \right) \sin(\omega_p t) \\ &+ 3H \left(\frac{m}{k_p} \right)^2 \cos(\omega_p t) \end{aligned} \right] + V_0^3 (t - 3H)
\end{aligned} \tag{15}$$

5.2. MATRIX FORM OF SEQUENTIAL RESPONSES

As the number of sequential responses increases it becomes increasingly difficult to solve them by hand due to the increased complexity of the equations. However, there are several patterns that emerge in the solutions that can be used to develop a general expression for the solutions. The resulting expression describing the solutions to all of the sequential responses is provided as a matrix equation in equation (16). The matrices in equation (16) reflect the patterns that emerge in the sequential response equations relating to phase shift, orders of t , and their respective coefficients.

$$\begin{bmatrix} x_1(t) \\ x_2(t) \\ \vdots \\ x_N(t) \end{bmatrix} = \mathbf{O}_w \left[\mathbf{W}_G \mathbf{L}_{G,x}(t) + \mathbf{W}_H \mathbf{L}_{H,x}(t) \right] + \mathbf{S}_x(t) \tag{16}$$

$\mathbf{S}_x(t)$ is the linear component of the solutions and is calculated in equation (17), where N is the maximum number of part rotations to be modeled.

$$\mathbf{S}_x(t) = \begin{bmatrix} V_0 (t - H) \\ V_0^2 (t - 2H) \\ \vdots \\ V_0^j (t - jH) \end{bmatrix} \quad j = 1, 2, \dots, N \tag{17}$$

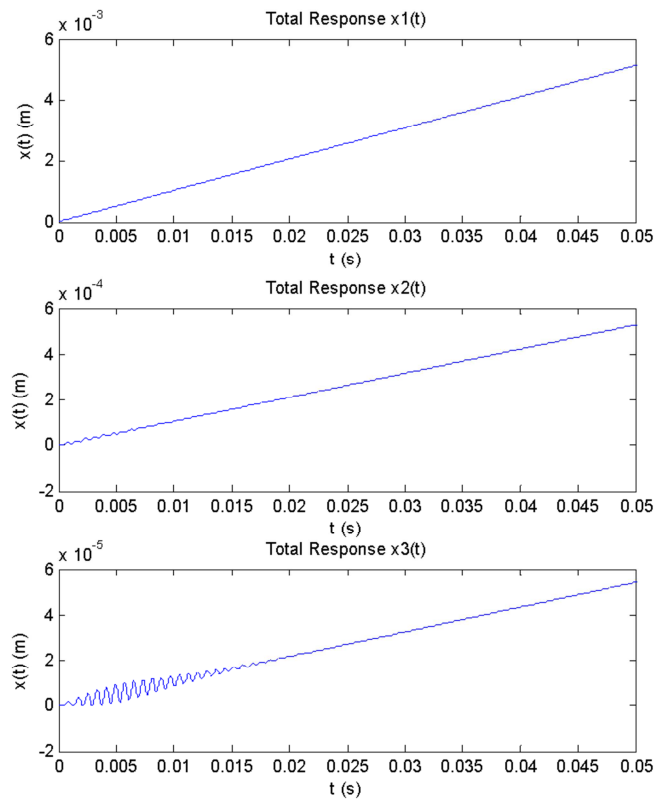


Fig. 10. Plots of the first three sequential responses described in equation (15)

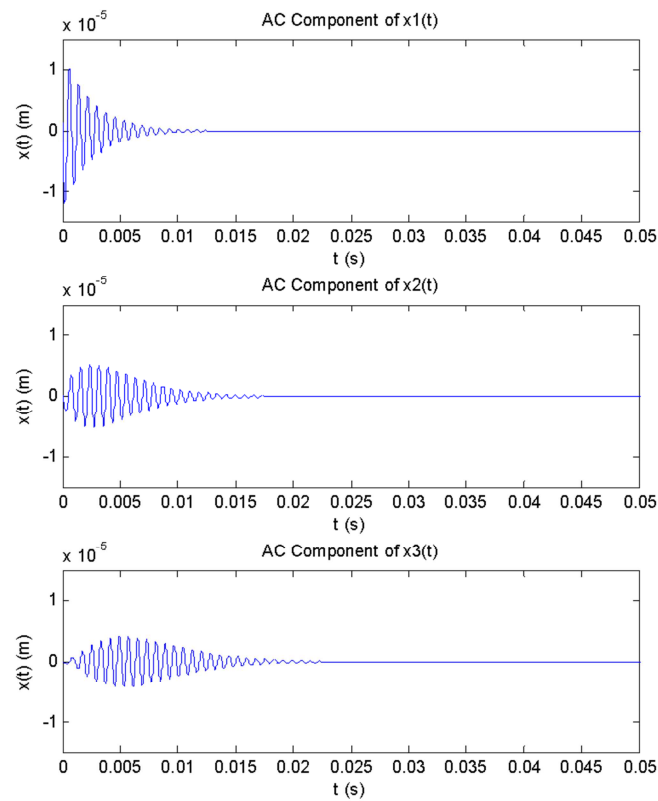


Fig. 11. AC components of the first three sequential response functions

The \mathbf{W} and \mathbf{L} matrices piece together the sine and cosine terms with the correct order of t and phase shift (equation (18)) with the corresponding coefficient (equations (19)). The G and H subscripts indicate which initial constant the matrices are associated with.

$$\mathbf{L}_{G,x}(t) = \begin{bmatrix} e^{-At} \sin(\omega_p t) \\ te^{-At} \sin\left(\omega_p t - \frac{\pi}{2}\right) \\ \vdots \\ t^{j-1} e^{-At} \sin\left(\omega_p t - (j-1)\frac{\pi}{2}\right) \end{bmatrix}_{j=1,2,\dots,N} \quad (18)$$

$$\mathbf{L}_{H,x}(t) = \begin{bmatrix} e^{-At} \cos(\omega_p t) \\ te^{-At} \cos\left(\omega_p t - \frac{\pi}{2}\right) \\ \vdots \\ t^{j-1} e^{-At} \cos\left(\omega_p t - (j-1)\frac{\pi}{2}\right) \end{bmatrix}_{j=1,2,\dots,N}$$

The coefficients of the \mathbf{W} matrices are calculated based on their position in the matrix. The diagonal terms, which are associated with the highest order of t for the for the j th sequential response, are calculated using equation (20). The coefficients of the first columns of the \mathbf{W} matrices, which are associated with the t of order zero, are calculated using equation (21). The remaining lower triangle coefficients are calculated using equation (22), and the upper triangle coefficients are all zero.

$$\mathbf{W}_G = \begin{bmatrix} W_{G1,1} & 0 & 0 & 0 \\ W_{G2,1} & W_{G2,2} & 0 & 0 \\ \vdots & W_{G3,2} & \ddots & 0 \\ W_{Gj,1} & W_{Gj,i} & \cdots & W_{Gj,j} \end{bmatrix}_{j,i=1,2,\dots,N} \quad (19)$$

$$\mathbf{W}_H = \begin{bmatrix} W_{H1,1} & 0 & 0 & 0 \\ W_{H2,1} & W_{H2,2} & 0 & 0 \\ \vdots & W_{H3,2} & \ddots & 0 \\ W_{Hj,1} & W_{Hj,i} & \cdots & W_{Hj,j} \end{bmatrix}_{j,i=1,2,\dots,N}$$

$$W_{Gj,j} = \frac{G}{(j-1)!(2\omega_p)^{(j-1)}} \quad (20)$$

$$W_{Hj,j} = \frac{H}{(j-1)!(2\omega_p)^{(j-1)}}$$

$$W_{Gj,i} = \frac{1}{\omega_p} \left(\mathbf{W}_{Gj,i+1} - \left(\frac{m}{k_p} \right)^{j-1} \right) \quad (21)$$

$$W_{Hj,i} = H j \left(\frac{m}{k_p} \right)^{j-1}$$

$$W_{Gj,i} = \frac{1}{2\omega_p(i-1)} [i(i-1)W_{Gj,i+1} + W_{Gj-1,i-1}] \quad (22)$$

$$W_{Hj,i} = \frac{1}{2\omega_p(i-1)} [i(i-1)W_{Hj,i+1} + W_{Hj-1,i-1}]$$

Finally, the coefficient in front of the oscillating terms is accounted for by \mathbf{O}_w as shown in equation (23).

$$\mathbf{O}_w = \begin{bmatrix} V_0 & 0 & 0 & 0 \\ 0 & V_0 \left(\frac{bR}{m} \right) & 0 & 0 \\ 0 & 0 & \ddots & 0 \\ 0 & 0 & 0 & V_0 \left(\frac{bR}{m} \right)^{j-1} \end{bmatrix}_{j=1,2,\dots,N} \quad (23)$$

6. NUMERICAL SOLUTION COMPARISON

The analytical time domain solution developed in this paper is compared with numerical simulated results for a simple turning operation. The system parameters used for the turning examples are provided in Table 1.

Table 1. System parameters used for the turning examples

k	5E7 N/m
m	0.88 kg
c	663.325 Ns/m ($\xi = 0.05$)
K_s	2E9 N/m ²
B	70 degrees
Feed per rev	0.076 mm (0.003 inch)

The two examples used for comparison are shown on the system stability lobe diagram in Fig. 12, where example 1 is expected to be unstable, and example 2 is expected to be stable. Example 1 has a spindle speed of 2000 rpm ($\tau=0.03s$), in example 2 the spindle speed is 12000 rpm ($\tau=0.005s$), and in both examples the depth of cut, b , is set at 10% above $b_{lim,crit}$.

In both examples the analytical response is found by applying the sequential responses in equation (16) to the double ramp turning model in equation (12). The results from Fig. 13 show the positional response, $x(t)$, from the analytical model and the numerical simulation. The positional responses shown here are the tool displacements relative to the nominal position of the tool, which eliminates the global linear feed of the tool during the operation. The results from Fig. 13 show that the response from the analytical solution closely matches the response from the numerical simulation. However, the dominance of the linear component of the response makes it difficult to see details of the AC component responses. In Fig. 14 the acceleration responses are shown for example 1 to eliminate the linear component, where the acceleration sequential responses, $acc(t)$, are derived by differentiating the positional sequential responses, $x(t)$, twice. Here again, the vibrational component of the tool tip response using the analytical solution matches that of the numerical solution.

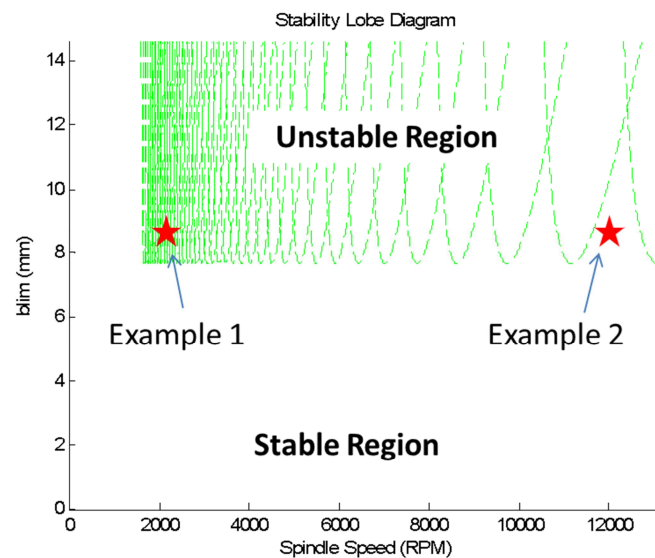


Fig. 12. Two examples shown on a stability lobe diagram, where example 1 is unstable, and example 2 is stable

The time domain responses for the two examples shown in Fig. 14 and Fig. 15 were obtained by applying the sequential response accelerations to equation (12). This process is illustrated in Fig. 17, where the individual acceleration components of the sequential responses are plotted along with the total acceleration response for both examples. Because the depth of cut, b , is the same in both examples, the individual acceleration responses which combine to generate the total response are the same for both examples. As such, the only significant difference between the two examples is the value of the time delay, τ .

In example 1 $\tau=0.03s$, corresponding to a spindle speed of 2000RPM, and the individual vibration pulses are spread out far enough in time that there is little interaction between them, and each pulse can be easily observed in the total response. The lack of interaction in example 1 between the individual pulses means that the trend of the total response will follow the trend of the individual responses (i.e. if the amplitudes of the individual vibrations grow, so will the total response).

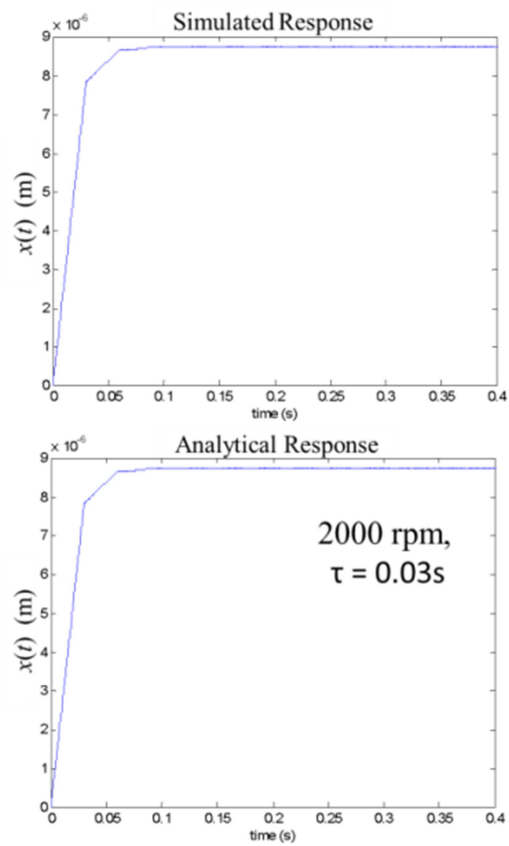
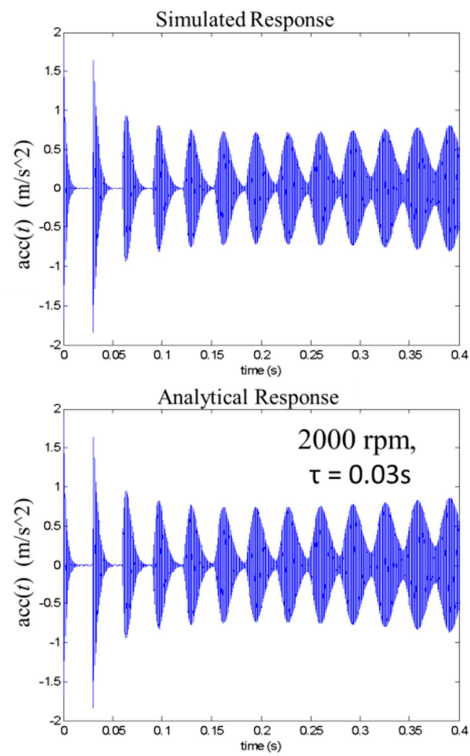
Fig. 13. Simulated and analytical positional response, $x(t)$, for Example 1

Fig. 14. Analytical and numerical acceleration responses for example 1

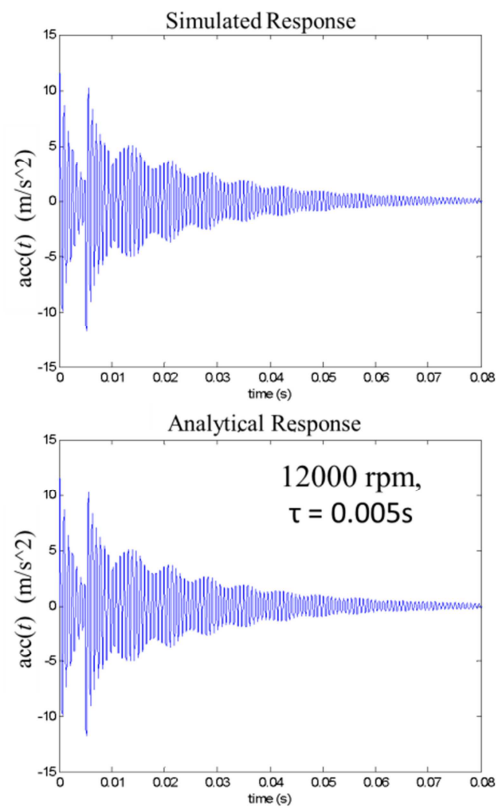


Fig. 15. Analytical and numerical acceleration responses for example 2

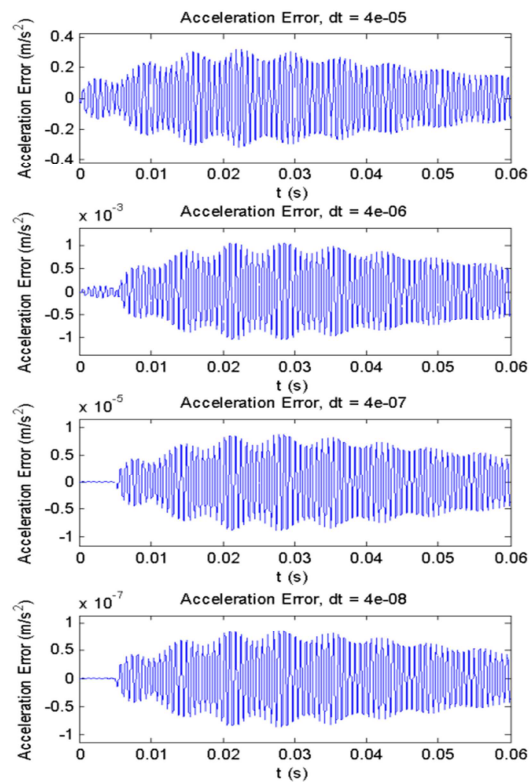


Fig. 16. Difference errors between the analytical and numerical acceleration responses for example 2 for multiple time step sizes

In example 2, τ is much smaller due to higher spindle speed, and the individual vibration pulses have significant overlap. The resulting interactions between the multiple vibration pulses have a cumulative constructive or deconstructive interference effect, which causes the total response to be stable or unstable depending on the value of τ . In example 2, the cumulative destructive interference between the multiple vibration pulses create a circumstance where the total response has decreasing amplitude with time while the individual acceleration vibrations increase over time.

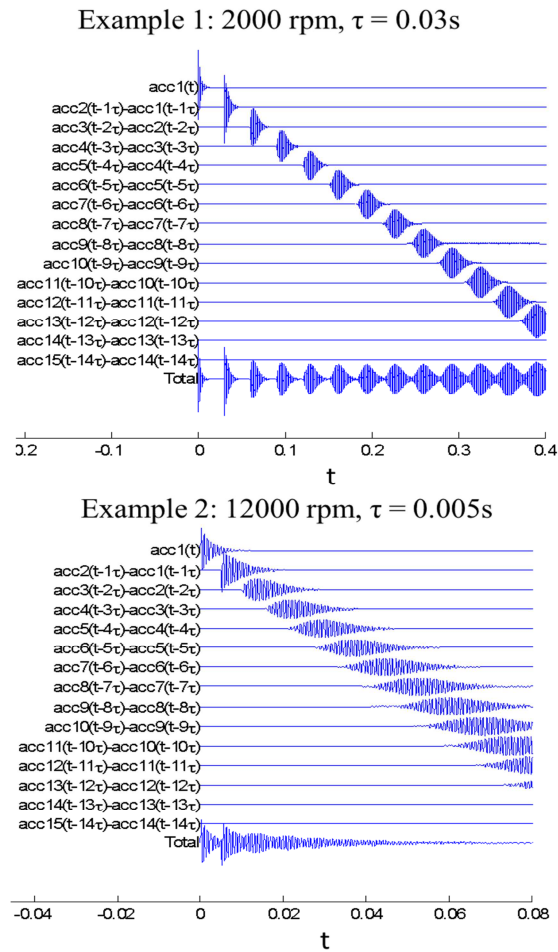


Fig. 17. Illustration of how the total tool tip response is generated from the sequential responses

7. CONCLUSION

An analytical model was developed to describe the time domain response of a tool during a simple turning operation. The method relies on superposition to construct a total dynamic response from a fixed set of individual, sequential responses. These sequential responses stem from some initial excitation event (input ramp function in this derivation) which propagates over time through repeated self-excitation. The resulting dynamic response of the system as a whole is found as a combination of the sequential responses

applied at different points in time based on the time delay term, τ . This solution approach provides some insight as to the cause of instability from a time domain perspective, where the global behavior is a result of constructive or deconstructive interference between many vibration pulses which propagate over time. Currently, this approach has shown to be effective for continuous cutting in turning based on comparisons with numerical simulations.

REFERENCES

- [1] ALTINTAS Y., BUDAK E., 1995, *Analytical prediction of stability lobes in milling*, Annals of CIRP, 44/1.
- [2] BAYLY P.V., HALLEY J.E., MANN B.P., DAVIES M.A., 2003, *Stability of interrupted cutting by temporal Finite Element Analysis*, Journal of Manufacturing Science and Engineering, 125/2, 220–225.
- [3] DAVIES M.A., PRATT J.R., DUTTERER B., BURNS T. J., 2002, *Stability prediction for low radial immersion milling*, Journal of Manufacturing Science and Engineering, 124, 217–225.
- [4] INSPERGER T., STEPAN G., 2002, *Semi-discretization method for delayed systems*, International Journal for Numerical Methods in Engineering, 55/5, 503–518.
- [5] INSPERGER T., STEPAN G., 2004, *Updated semi-discretization method for periodic delay differential equations*, International Journal for Numerical Methods in Engineering, 61, 117–141.
- [6] MERDOL S.D., ALTINTAS Y., 2004, *Multi frequency solution of chatter stability for low immersion milling*, Journal of Manufacturing Science and Engineering, 126, 459–466.
- [7] MYSHKIS A.D., 1998, *Differential equations, ordinary with distributed arguments*, Encyclopedia of Mathematics, Boston, Kluwer Academic Publishers, 3, 144–147.
- [8] OZOEGWU C.G., OMENYI S.N., 2012, *Time domain chatter stability comparison of turning and milling processes*, International Journal of Multidisciplinary Sciences and Engineering, 3/11, 25.
- [9] SCHMITZ T.L., SMITH K.S., 2009, *Machining dynamics - frequency response to improved productivity*, New York, NY, Springer.
- [10] SHAMPINE L.F., THOMPSON S., 2001, *Solving DDEs in Matlab*, Applied Numerical Mathematics, 37, 441–458.
- [10] TLUSTY J., ISMAIL F., 1981, *Basic non-linearities in machining chatter*, Annals of CIRP, 30, 299–304.
- [11] TLUSTY J., POLACEK W., 1963, *The stability of machine tools against self excited vibrations*, ASME International Research in Productoin Engineering, 1, 465–474.